Approved, DCU# 43-7702-21

Notional Four-Zone MVDC Shipboard Cooling System Model

ONR GRANT # N00014-16-1-2956

Model Description Document
Prepared by ESRDC Team at
Center for Advanced Power Systems
Florida State University
January 19, 2021

FLORIDA STATE UNIVERSITY
CENTER FOR ADVANCED POWER SYSTEMS

MISSION STATEMENT

The Electric Ship Research and Development Consortium brings together in a single entity the combined programs and resources of leading electric power research institutions to advance near- to mid-term electric ship concepts. The consortium is supported through a grant from the United States Office of Naval Research.

REVISION HISTORY

Version	Date	Pages	Comment
1.0	06/01/20	All	Initial version of the document
2.0	07/27/20	All	Revised model and notional parameters; transition from Word to LaTeX
2.1	07/29/20	Section 3.3.1, 4.3, and 5	Minor revision
2.2	08/04/20	Section 2	Added hierarchy figure (Figure 1); changed page margin; minor revision
2.3	12/01/20	Appendix A	Updated equipment list
2.4	01/19/21	All	Revised after an external review

Contents

Acronyms

ACLC	AC load center
CONV	Converter
ESM	Energy storage module
ESRDC	Electric Ship Research and Development Consortium
HVAC	Heating ventilation and air-conditioning
IPNC	Integrated power node center
MDD	Model description document
ML	Mission load
MVDC	Medium voltage DC
PCM1A	Power conversion module
PGM	Power generation module
PMM	Propulsion motor module
RECT	Rectifier
RTS	Real time simulator
sRTS	Soft-Real time simulator
STBD	Starboard

Document Summary

The following document presents a notional four-zone medium voltage DC (MVDC) shipboard cooling system model formulated for piping network design, system-level thermal analysis, and co-simulation purposes. In particular, this model description document (MDD) elaborates on mathematical equations describing the complete notional four-zone ship cooling network along with modeling assumptions and pertinent numerical methods. The modelling approach employed herein incorporates all major thermal-fluid components present in any zone to ensure proper operation of corresponding thermal loads, and it is not bounded by a particular cooling network layout nor the number of thermal loads. The major thermal-fluid components treated herein are gate valves, pumps, pipes, chillers, and heat exchangers. The model is therefore expandable to a larger system as long as the considered assumptions remain valid and a similar fidelity is sought.

1 Introduction

The growing demand for high-power density shipboard equipment and resilience poses significant thermal management challenges with stringent operational and design constraints. The complex interdependence and functional correlation among disparate subsystems in an integrated power-thermal-fluid system aboard ships emphasize the need for its comprehensive assessments in early design stages to ensure proper operation of mission-critical components in all conceivable ship operating modes. Subsequently, case studies incorporating various mission profiles and what-if scenarios deserve a closer scrutiny for the development of accurate, reliable, and fast shipboard system health monitoring, prognosis, and control strategies.

The dependence of ship thermal-fluid design and operation on the electrical performance and power management entails the formulation of a holistic electrical-thermal-fluid model whose state variables such as power, conversion efficiency, temperature, and heat generation are closely coupled. The notional 4-zone MVDC shipboard power system model has been previously implemented in a real time simulation (RTS) environment [1], and we propose herein its complementary thermal-fluid model developed in MATLAB/Simscape by exploiting its built-in thermal-fluid component library. Furthermore, its physics-based modeling platform enables high-fidelity assessment and testing of realistic operating conditions and controls, respectively.

The goal of this MDD is to provide the basis for future shipboard cooling system models by presenting a generalized thermal-fluid model featuring all major cooling system components in a standard manner, i.e., independent of cooling network architecture or the number of thermal loads. The MDD may also serve as a reference during future implementations or extensions of similar models in various simulation platforms as the presented model is not platform specific. The MDD is organized as follows: Section 2 summarizes the specific goals of this MDD while Section 3 provides an overview of a notional four-zone MVDC ship cooling network and presents the mathematical model of each representative thermal-fluid model component along with modeling assumptions. Section 4 summarizes the numerical characteristics and numerical methods pertinent to the proposed model, and how these are associated with the development of a real-time co-simulation environment.

2 Purpose

The model presented herein is capable of capturing dynamic thermal-fluid responses across all four zones. The primary variables of interest are temperature, flow rate, and pressure. The purpose of this MDD can be summarized as follows:

- To present a generalized thermal-fluid model of a notional four-zone MVDC ship cooling system easily extensible to a larger system or different cooling configurations.
- To serve as a common ground for future implementations and extensions of similar models in various simulation platforms.
- To summarize numerical characteristics and pertinent methods.
- To contribute in various efforts under the ESRDC project aiming to study areas such as advanced control algorithms and strategies, health monitoring and prognosis, thermal hardware-in-the-loop, power and thermal management, etc.

2.1 Requirements

The model requires prior knowledge of the piping network and thermal load characteristics. Furthermore, the model presented herein is physics-based; that is, it can only be solved when physically viable initial and boundary conditions are provided. The model may need expert knowledge in this regard to function as intended.

The current model implementation requires MATLAB/Simulink. However, one of the objectives of this MDD is to provide mathematical equations that can be solved using any numerical solver and/or programming language.

2.2 Model components

The model comprises several sub-models representing different thermal-fluid components, namely thermal loads (equipment), pipes, valves, chillers, pumps, and expansion tanks. Thermal loads are electrical loads that dissipate heat and require external cooling; pipes connect two or more thermal-fluid components; valves are gate and check valves that control the amount and direction of fluid flow, respectively; chillers are refrigeration systems used to cool freshwater (coolant); pumps are hydraulic components that induce fluid flow; and expansion tanks serve to absorb excess fluid pressure caused by thermal expansion.

2.3 Model hierarchy

The present shipboard cooling system model may be coupled to a shipboard power system model for co-simulations as illustrated in Figure 1, where all coupling variables are represented by green circles while controllers are denoted by yellow diamonds. While co-simulations typically involve RTS for power systems, the cooling system model may be solved alone simply by replacing the coupling variables with user-defined static or dynamic variables.

The flow control (gate) valves placed before each shipboard load is opened/closed according to the load temperature T (see Figure 1). Furthermore, these valves can be disabled to simulate cases wherein valves remain closed regardless of the temperature feedback, e.g., stuck closed valves. The current model implementation and co-simulation setup do not feature a separate control layer; instead, each physical system model has its own controllers as indicated in Figure 1. The mutual interaction between shipboard loads and controllers are discussed in detail and further illustrated in Section 3 and 5.

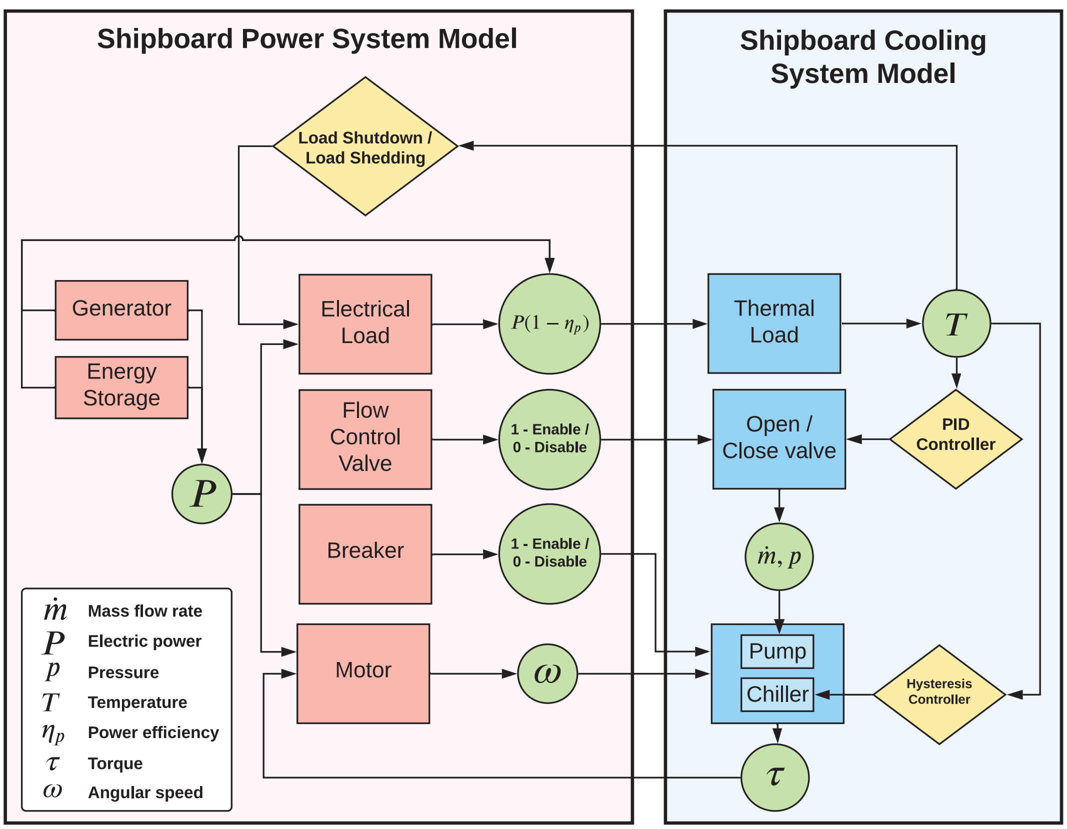

Figure 1: Model hierarchy where the arrows indicate the signal flow direction.

3 Mathematical Model

Figure 2 depicts a notional 4-zone MVDC ship cooling network with more than 50 anticipated thermal-fluid components. In this particular layout, the two sides, port and starboard, and the neighboring zones are cross connected via supply and return headers to introduce cooling redundancy. The gate valves placed in between enable the redistribution of cooling power among zones and sides based on available cooling power and demand. Similarly, check valves are placed after each load to prevent backflow. The thermal loads in Figure 2 are connected to the main supply and return headers via branches, each with its own gate valve to control coolant mass flow rate and thus the supplied cooling power. The cooling network features two centrifugal pumps and chillers per zone (one on each side), and it can be extended to encompass additional water-cooled equipment or an HVAC system.

3.1 Piping network

The bypass line parallel to the chiller is used only during the maintenance period or in case of an emergency. Salient features of the notional cooling network under consideration are summarized as follows:

- **Flexible:** Expandable to a larger network, e.g., add more zones, components, etc.
- **Reconfigurable:** Pipes can be easily added or removed depending on design requirements.
- **Redundant:** Interconnection of sides and zones provides an extra layer of resilience during abnormal conditions, e.g., allocation of remaining cooling power from Port side to STBD side when STBD side losses its cooling capability.

The network is fully instrumented to monitor temperatures, pressures, and mass flow rates across the system as well as pump and chiller power consumption and valve openings.

3.2 Model capabilities

The proposed model features the following thermal-hydraulic characteristics and capabilities some of which can be easily enabled and disabled. Note that model complexity (and thus the computational cost) increases along with its capability.

- Fluid compressibility can be included or excluded depending on modeling needs and applications.

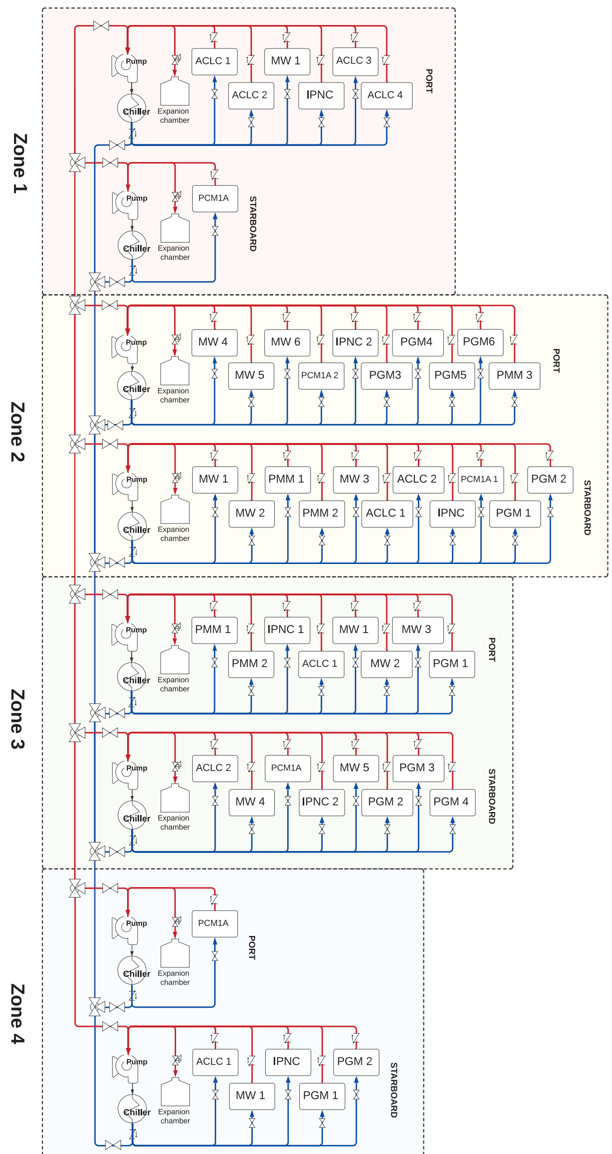

Figure 2: Notional four-zone MVDC ship zone cooling network where each zone comprises a chiller & pump set, cross-connected sides, expansion chamber, and loads. Here ACLC—AC load center; MW—Megawatt load; IPNC—integrated power node center; PCM1A—power conversion module; PGM—power generation module; and PMM—propulsion motor module.

- Fluid inertia can be included or excluded depending on modeling needs. The inertial force on the fluid, however, is typically neglected at the large time scales over which flow variations occur.

- Thermal inertia of shipboard equipment, which accounts for dynamic thermal response, can be included or excluded alike fluid inertia. Shipboard loads are modeled based on the lumped capacitance approach which is elaborated in the following section.
- Three major heat transfer mechanisms—conduction, convection, and radiation which are quantified based on existing empirical correlations (e.g., Gnielinski correlation for convection in turbulent pipe flow) or analytical equations.
- Minor head losses (local resistance) due to pipe fittings, bends, and hydraulic components and major head loss due to viscous friction given by Haaland or Darcy-Weisbach equation.
- Spatiotemporal mass, pressure, and temperature variations across the piping network.

Subsequently, the following physical events relevant to piping networks can be simulated with the proposed model:

- Pipe leak following the conservation of mass and removing fluid mass from the system.
- Reverse flow following the conservation of momentum forcing fluid to move from high pressure to low pressure region in absence of external force such as that from a pump.
- Chiller or pump failure by cutting off power which could occur during load shedding.
- Valve malfunction by overriding valve controllers and forcing them to remain shut or open which hampers both shipboard component and system-level cooling.
- Redistribution of cooling power across ship sides (port and starboard) via cross-connection valves in case of cooling system failure or increased cooling demand from particular cooling sections.

3.3 Model formulation

The thermal-fluid model is formulated based on the conservation laws, namely mass, momentum, and energy given as follows in a control volume form:

$$\frac{dm}{dt} = \sum_{in} \dot{m} - \sum_{out} \dot{m}, \tag{1}$$

$$\frac{d}{dt}\int_V \mathbf{u}\rho dV = \sum_{in} \dot{m}\mathbf{u} - \sum_{out} \dot{m}\mathbf{u} + \sum_{ext} \mathbf{F}, \tag{2}$$

and

$$\rho V c_p \frac{dT}{dt} = \dot{Q} - \dot{W} + \sum_{in} \dot{m}h - \sum_{out} \dot{m}h + \sum \dot{Q}_s, \tag{3}$$

where m and $\dot{m}$ are mass and mass flow rate; t is time; $\mathbf{u}$, ρ, and V are velocity, density, and volume, respectively; $\mathbf{F}$ is force; c_p, $\dot{Q}$, $\dot{W}$, and h are specific heat, heat generation rate, power, and enthalpy, respectively. The subscript s denotes source. These three equations are invoked and simplified throughout the rest of this section as the model of each shipboard thermal-fluid component is presented.

The model is simplified using the lumped capacitance approach, wherein uniform thermodynamic properties (e.g., temperature, internal energy, specific heat, etc.) are assumed for each control volume. Analogously, this can be regarded as a single capacitor representing a battery pack. This approach has been demonstrated to yield a simple yet sufficiently accurate model of ship cooling systems (refer to Ref. [2]) or any component with a large thermal inertia and small internal thermal resistance.

Most equations and a large portion of descriptions given in this section have been excerpted from Ref. [3] as the proposed cooling system model is heavily based on MATLAB/Simulink platform.

3.3.1 Thermal load

Figure 3 illustrates a lumped control volume representing a ship thermal load subject to heat and mass transfer, where $\dot{Q}_{conv}$ is the convective heat transfer between load i and freshwater (fw). The arrows indicate the coolant flow direction, and the gate valve controls the freshwater flow rate according to how much load temperature T_i deviates from the prescribed operating temperature. The gate valve model is described in Section 3.3.3.

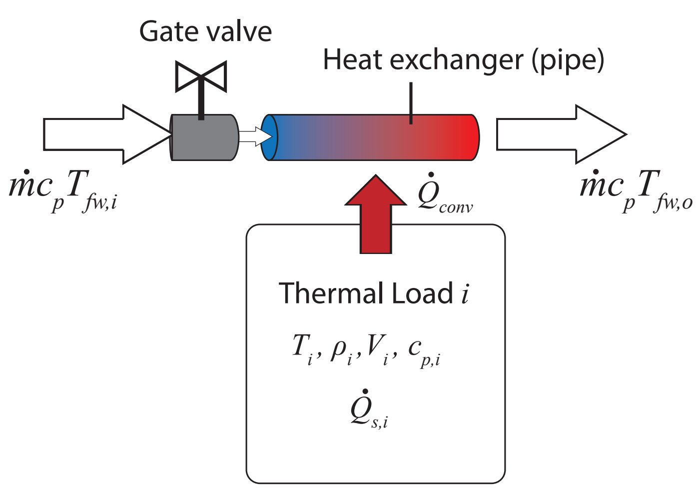

Figure 3: Illustration of a thermodynamic control volume representing a load.

The conservation of mass and momentum do not apply to load i as no mass crosses the control volume. Furthermore, Eq. (3) can be simplified to

$$(\rho V c_p)_i \frac{dT_i}{dt} = -\dot{Q}_{conv} + \dot{Q}_{s,i}, \tag{4}$$

where the internal heat generation $\dot{Q}_{s,i}$ is the product of corresponding dynamic load power $P_{e,i}$ and its power conversion efficiency $\eta_{p,i}$, i.e., $\dot{Q}_{s,i} = P_{e,i}\,(1 - \eta_{p,i})$ where both $P_{e,i}$ and $\eta_{p,i}$ are typically time-dependent. $\dot{Q}_{s,i}$ may be defined by an analytical function, tabulated data, or as a constant in standalone (not real-time co-sim) simulations. In real-time co-simulations, $\dot{Q}_{s,i}$ is provided by the SPS model whose $P_{e,i}$ and $\eta_{p,i}$ follow prescribed mission profiles. The standalone case in an automated test framework (test harness) is elaborated further in the model user guide (see Ref. [4]). Each load heat exchanger is represented by a pipe as indicated in Figure 3 and elaborated in Section 3.3.2.

3.3.2 Pipe

Pipes are considered adiabatic, rigid, and quasi-steady, and minor losses such as entrance effect, elbows, and junctions are accounted by local resistance values (as an aggregate equivalent length). Every pipe in the network can be discretized into smaller segments, and the appropriate number of pipe segments to consider depends on the time scales over which temperature and pressure propagate through the pipe [3]. In addition, space-varying thermal boundary condition may require segmented pipes for proper interactions.

The conservation of mass in Eq. (1) applied to pipe segment volume i yields

$$\rho_i \frac{dV}{dt} + \rho_i V \left(\frac{1}{\gamma_i} \frac{dp_i}{dt} - \alpha_i \frac{dT_i}{dt} \right) = \dot{m}_{in} - \dot{m}_{out}, \tag{5}$$

where γ and α denote the bulk modulus and thermal expansion coefficient, and p is the average flow pressure. The first term on the left accounts for a flexible pipe or mass accumulation while the term inside the parenthesis models the fluid dynamic compressibility, in which case the fluid mass within a pipe changes as a function of pressure and temperature. The pressure drop across each pipe segment can be obtained as

$$\Delta p = p_{in} - p_{out} + \rho g \Delta z; \tag{6}$$

where Δz is the spatial discretization along the pipe length. Nonlinear pressure variation along the pipe can be modeled by splitting Eq. (6) over two or more control volumes, e.g., one for each pipe half.

The energy balance applied to pipe segment volume i results in

$$\rho_i V \left[\frac{d\vartheta}{dp}\frac{dp}{dt} + \frac{d\vartheta}{dT}\frac{dT}{dt} \right]_i + (\rho_i \vartheta_i + p_i) \left(\frac{dV}{dt} \right)_i = (\dot{m}h)_{in} - (\dot{m}h)_{out} + \dot{Q}_{conv,j}, \tag{7}$$

in which ϑ and h are the specific internal energy and enthalpy, while $\dot{Q}_{conv,j}$ is the convective heat transfer between cooling medium and shipboard equipment j. If fluid dynamic compressibility and pipe expansion (or mass accumulation) are neglected, Eq. (7) simplifies to

$$(\rho V c_p)_i \frac{dT_i}{dt} = (\dot{m}h)_{in} - (\dot{m}h)_{out} + \dot{Q}_{conv,j} \tag{8}$$

since $\vartheta = c_p T$ in the incompressible substance limit and the fluid enthalpy is given by $h = \vartheta + pV$ or $h = c_p T$ for an incompressible flow. The temperature is assumed to vary exponentially along the pipe while neglecting conduction across the pipe wall. As a result, $\dot{Q}_{conv,j}$ between pipe segment volume i and shipboard load j is expressed in its general form as

$$\dot{Q}_{conv,j} = \dot{m}c_p \left(T_j - T_{i,in}\right) \left[1 - e^{-(UA_{ht})_{ij}/(\dot{m}c_p)}\right], \tag{9}$$

Here U is the overall heat transfer coefficient given by a constant (laminar flow) or empirical correlation such as Dittus-Boelter or Gnielinski correlation (turbulent flow).

We neglect radiative heat transfer and any thermal interaction between a pipe segment and its surroundings in the notional four-zone MVDC cooling system as shipboard piping network is well-insulated. Eq. (9) is used to find $\dot{Q}_{conv}$ in Eq. (4). In case there are multiple pipe segments (e.g., a supply header discretized into N segments), Eqs. (5)–(7) are solved for each segment and the mass, momentum, and energy transfer between segments are quantified accordingly.

3.3.3 Valve

Gate valves are placed before every ship load as well as in between zones and sides to control flow with a circular opening and a circular gate as illustrated in Figure 4. The figure shows how the gate valve positions vary from fully closed to fully opened case (Figure 4 was excerpted from Ref. [3]).

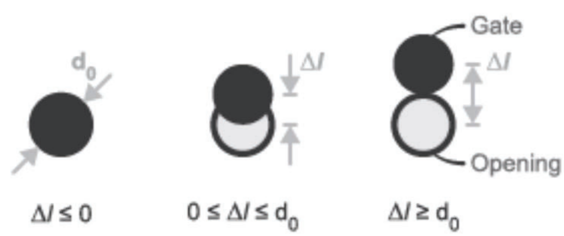

Figure 4: Gate valve in different positions [3].

The valve opening area (A) is given by

$$A = \frac{\pi d_0^2}{4} - A_{closed} \tag{10}$$

in which d_0 is the valve orifice diameter while A_{closed} is the portion of A covered by the gate. A_{closed} is obtained as [3]

$$A_{closed} = \frac{d_0^2}{4} \arccos\left(\frac{\Delta I}{d_0}\right) - \frac{\Delta I}{2}\sqrt{d_0^2 - (\Delta I)^2}. \tag{11}$$

In Eq. (11), ΔI is the net displacement of the gate center with respect to the orifice center. Eqs. (10) and (11) introduce numerical discontinuity as the opening area may change abruptly as a step function. This problem is mitigated by smoothing the valve opening area variation between the two extreme positions using a polynomial function. In principle, one can use Sigmoid functions for a smooth transition.

The momentum balance across the valve yields [3]

$$\Delta p = \frac{\dot{m}\sqrt{\dot{m}^2 + \dot{m}_{crit}^2/d}}{2\rho c_d^2 S^2}\left[1 - \left(\frac{A}{S}\right)^2\right]\beta, \tag{12}$$

where $\dot{m}_{crit}$, c_d, S, and β are critical mass flow rate, discharge coefficient, valve inlet area, and pressure loss coefficient, respectively. The critical mass flow rate is given by

$$\dot{m}_{crit} = \mathrm{Re}_{cr}\mu\sqrt{\frac{A\pi}{4}} \tag{13}$$

in which Re_{cr} and μ are critical Reynolds number and average dynamic viscosity of fluid.

Check valves are modeled in a similar manner by modifying gate valve control mechanism. Instead of relying on an external temperature-feedback controller, check valves are controlled based on inlet and outlet pressure difference—valves close when the difference is negative (outlet pressure greater than that of the inlet and vice-versa).

3.3.4 Chiller

The development of a numerically stable, accurate, and computationally efficient vapor compression refrigeration system model remains as a challenge as it involves three distinct refrigerant phases (i.e., subcooled, two-phase, and superheated) as well as refrigerant expansion and compression. Moreover, the integration of such a sophisticated model into a comprehensive system-level model may introduce numerical instability and control issues. As a result, the proposed generalized model treats the chiller as a quasi-steady single-stream heat exchanger (pipe) capable of removing enough heat to provide the desired supply temperature $T_{fw,s}$. Figure 5 depicts the simplified chiller model schematic where the coefficient of performance (COP) is assumed known a priori to obtain the compressor power required to drive the chiller, $\dot{W}_{comp}$. The subscripts s and r denote supply and return, respectively.

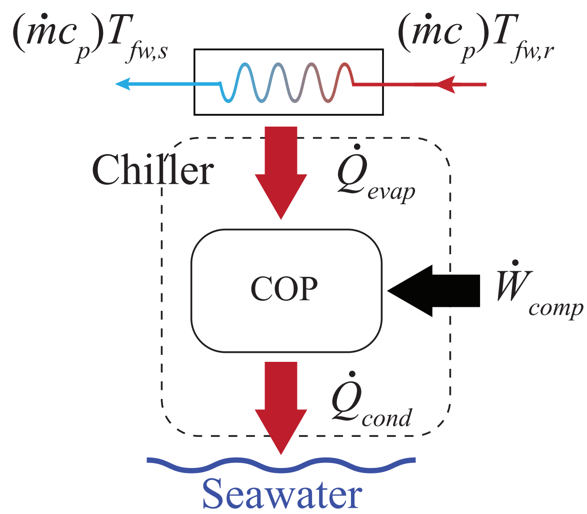

Figure 5: Schematic of the simplified chiller model.

The amount of heat that must be removed from the coolant stream is given by the following energy balance since the setpoint temperature ($T_{fw,s}$) is prescribed:

$$\dot{Q}_{evap} = \dot{m}c_p \left(T_{fw,r} - T_{fw,s}\right) \tag{14}$$

or by Eq. (9) with constant evaporator wall temperature and variable thermal resistor (which becomes large when the chiller is off and vice-versa) as the chiller evaporator is represented by a pipe in our model. Subsequently, the compressor power is obtained as $\dot{W}_{comp} = \dot{Q}_{evap}/\mathrm{COP}$ where COP is a ratio of useful heating or cooling provided to work required. Since the chiller is not explicitly modeled herein, its dynamic response is modeled by a second order transfer function. Furthermore, the operation of chiller (i.e., on-off cycles) is controlled with a hysteresis controller to ensure the actual coolant temperature at the chiller outlet remains within the predefined setpoint (desired) temperature limit.

3.3.5 Pump

Pumps are considered adiabatic and quasi-steady in the proposed model, and they are modeled as centrifugal pumps based on the efficiency curves provided by manufacturers. The efficiency curves are obtained by determining the minimum mass flow rate required to cool all shipboard equipment under consideration as well as the total pressure drop across the pertinent piping network. The selected pump data are then referenced by the model as tabulated data comprising pump capacity (volumetric flow rate), head (Δh), and power ($\dot{W}_p$, impeller shaft power). Figure 6 depicts the centrifugal pump performance curve referenced by the present notional four-zone MVDC shipboard cooling system model.

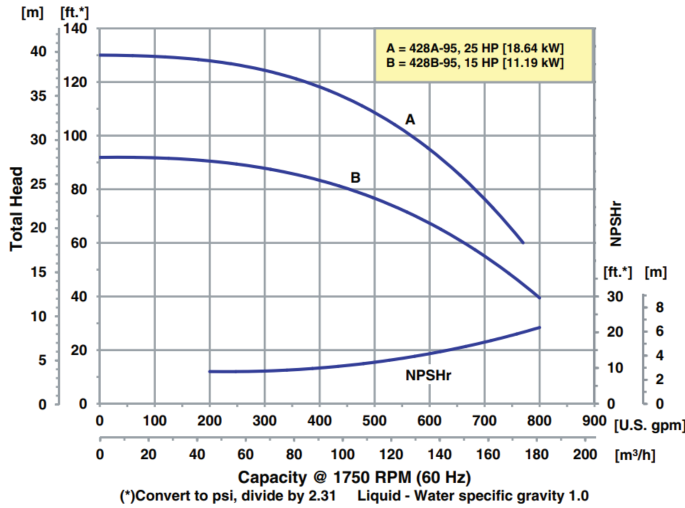

Figure 6: Centrifugal pump performance curve.

The pressure rise across the pump is computed as

$$\Delta p = \frac{\omega^2}{\omega_R^2} \rho g \Delta h, \tag{15}$$

where ω and ω_R are shaft speed and its reference value, respectively. The shaft speed can be provided by (1) the shipboard power systems model in case of co-simulation; (2) incorporating motor models into the proposed generalized model; or (3) assigning a constant value. The shaft torque is then computed as $\tau = \dot{W}_p/\omega$ where $\dot{W}_p$ is the pump breaker power.

3.3.6 Expansion tank

Expansion tanks are crucial elements of cooling networks as they prevent over-pressurization of coolant as its temperature rises. The expansion tank is modeled as follows:

$$p_{in} + p_{dyn} = p_i + \rho g \left(y - y_{in} \right), \tag{16}$$

and

$$\left(\rho V \right)_i \left(c_p + h\alpha \right) \frac{dT_i}{dt} = \left(\dot{m} h \right)_{in} + \dot{Q}_i, \tag{17}$$

where the positive pressure difference between the supply header and tank (i.e., $p_{in} - p_i > 0$) forces the pressurized water to enter the tank. Here p_{dyn} is the dynamic pressure and is nonzero only when there is mass leaving tank i, in which case $p_{dyn} = \dot{m}_{in}^2/(2\rho A_{in}^2)$. y_{in}, and A_{in} are tank inlet elevation relative to its bottom and inlet cross-section area, respectively. y is the tank height relative to the bottom, and T is the tank fluid temperature.

The energy balance in Eq. (17) can be simplified further by neglecting any thermal interaction between tank i and its surrounding, i.e., $\dot{Q}_i = 0$.

3.4 Ongoing modeling efforts

We constantly strive for a more versatile, accurate, and computationally efficient shipboard cooling system model. This section describes ongoing efforts, including model formulation and testing, to expand the proposed model capabilities and will be supported in future releases.

3.4.1 Interconnected zones

We are currently extending the existing notional piping network to interconnect all four zones for cooling power redistribution in case of a zone failure. The main idea is similar to the cross-connected sides (Between Port and STBD) featured by the current model, but an effective means to control interconnection flow valves and to quantify the cooling power drawn from fully-functional zones is being investigated.

3.4.2 Ship compartment

The thermal interaction between shipboard equipment and its surroundings, e.g., compartment, can be as significant as that between ship cooling network components. The inclusion of such thermal interactions enables for a holistic thermal analysis like the prediction of minimum compartment HVAC loads or the assessment of the effects of shipboard equipment placement and location on thermal management strategies. Ship compartments are typically designed to withstand harsh thermal conditions while allowing crews to reside for a certain time period during equipment operation and maintenance. Furthermore, compartments may also be designed to provide additional cooling by retaining its temperature below that of equipment for heat rejection. Figure 7 illustrates the discussed thermal interaction between a shipboard component and its corresponding compartment.

The component-compartment thermal interaction modeling entails solving an additional ordinary differential equation for compartment ($comp$) given as

$$(\rho V c_p)_{comp} \frac{dT_{comp}}{dt} = UA\,(T_{load} - T_{comp}) + (\dot{m}c_p)_{air}(T_{air} - T_{comp}), \tag{18}$$

which is similar to Eq. (3) according to the lumped capacitance approach. Here T_{load} is the apparent equipment exterior temperature (T_{MW} in Figure 10); T_{comp} is the compartment air temperature; and T_{air} refers to the temperature of chilled air supplied from a chilled

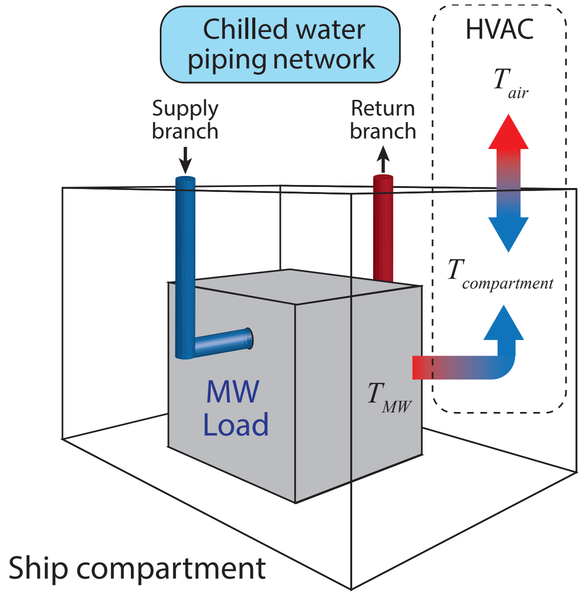

Figure 7: Illustration of shipboard component-compartment thermal interaction.

air handler via ducts. UA is the equipment thermal conductance describing the convection from load to compartment or vice-versa depending on the sign.

3.4.3 External model interface

The proposed generalized model may encompass components that cannot be modeled with sufficient accuracy using MATLAB/Simscape library components. As a result, the current modeling effort leaves room for potential integration of non-Simscape models such as those formulated using finite difference, finite element, or finite volume methods. In an effort to ensure fast numerical convergence, these models shall be incorporated as reduced-order models (e.g., ordinary differential equations, algebraic equations, etc.), response surface models, nonparametric models (Gaussian regression), or neural network models.

The external model interface is accomplished by using a MATLAB/Simulink system function (S-function) [3] which dynamically links Simulink models to Fortran, C, or C++ subroutines. In addition, numerous commercial software such as COMSOL Multiphysics and ANSYS offer MATLAB toolbox to facilitate the interface. The selection of an appropriate interface type (S-function or external toolbox) and the modeling approach (reduced-order, response surface, etc.) is up to the modeler's discretion based on the desired accuracy and the maximum allowed computational cost, which can be of critical importance in co-simulations wherein soft-RTS (sRTS) models must be solved faster than real time.

If the response surface method is selected, for example, the external model interface can be accomplished as follows:

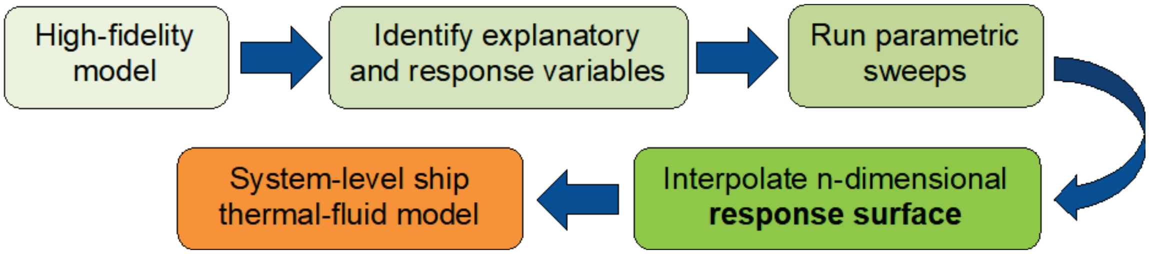

Figure 8: Flowchart of the high-fidelity model integration process using response surface method.

The response surface model obtained as in Figure 8 can then be called as a MATLAB function. If a COMSOL Multiphysics model is to be imported on the other hand, its built-in MATLAB interface can be used to load, modify, and simulate the model directly using a MATLAB script [5].

4 Numerical Requirements and Characteristics

4.1 Numerical requirements

Numerical accuracy, stability, and convergence must be considered for any numerical integration. These three characteristics often depend on the problem being solved and the constraints imposed by the computational grid or the types of equations under consideration. While numerous methods are available for a wide variety of problems, selecting an appropriate solver is often challenging, especially if the equations describing the model and their characteristics are not identified beforehand. The generalized model consists of ordinary differential equations (ODEs) resulting from the lumped capacitance approach and algebraic equations describing thermal-fluid components whose inertia is neglected.

The system of ODEs derived from the model presented in Section 4 is stiff if the solution being sought varies slowly while nearby solutions change rapidly; in other words, shipboard loads with drastically different transients (e.g., high ramp rate loads and non-vital loads) yield a system of stiff differential equations. Stiff systems are difficult to solve numerically; an explicit method must take small steps to retain numerical stability which in turn affects the numerical efficiency (and computational cost). An implicit method, on the other hand, has much greater stability region (or A-stable) which enables relatively larger time steps to be taken, but it re-quires additional equations to be solved using root-finding algorithms.

The selection of an appropriate numerical approximation for a problem entails choosing the right step size or predictor-corrector. Fixed-step solvers, for example, integrate the model at regular intervals from the beginning to the end of the simulation. A smaller step size generally increases the accuracy of the results but in exchange for increased computational time. In contrast, variable-step solvers feature dynamic step size controllers which reduce the step size to increase accuracy at certain iterations during the simulation and vice-versa. The proposed generalized thermal-fluid model comprises second-order transfer functions to avoid algebraic loops and numerical discontinuities. Each transfer function may have distinct time constant depending on the corresponding component dynamics.

4.2 Real-time co-simulation environment

The numerical approximation scheme and step size appropriate for real-time co-simulations must be carefully selected during the model development. However, the process of finding a suitable combination of model complexity, approximation scheme, and step size is heuristic to a large extent as the process is extremely problem-dependent. Finding the right balance between accuracy and simulation speed is critical—the model must be solved fast enough to avoid any overrun (when the model is not fast enough for real-time simulation) while retaining sufficient accuracy (recall computational speed and accuracy are incompatible). Figure 9 depicts the real-time model preparation workflow suggesting a structured way to identify the balance between speed and accuracy.

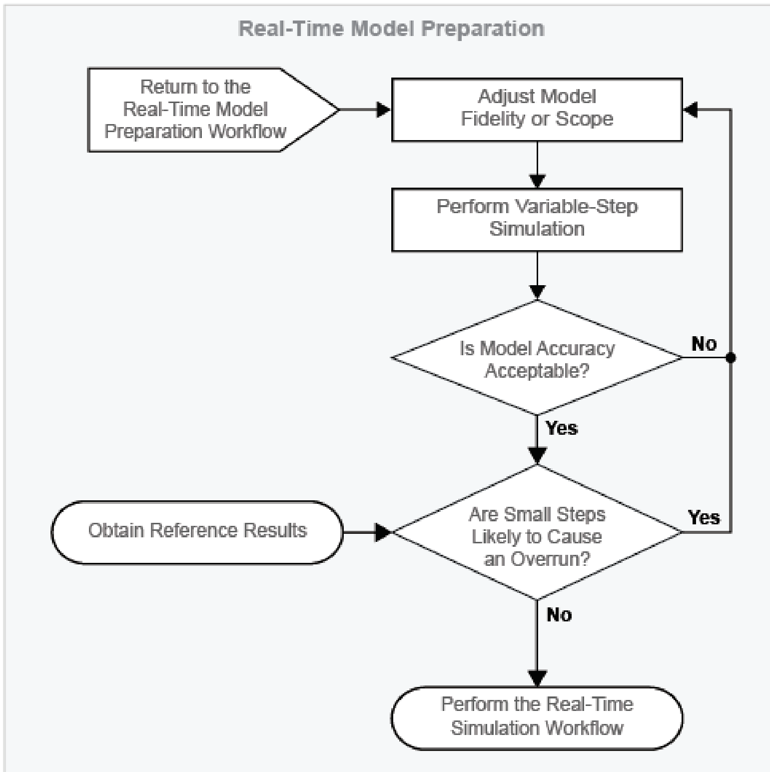

Figure 9: Real-time model preparation workflow [3].

After performing numerical experiments as illustrated in Figure 10, Backward Euler with a step size of 0.001 s was deemed appropriate for solving the proposed thermal-fluid model in a real-time co-simulation environment. Figure 6 verifies the accuracy of fixed-step solver against that of variable-step solver, according to which the considered fixed-step solver is able to accurately capture all system dynamics including those observed during start-up.

4.3 Model scalability

The model scalability is another crucial numerical characteristic that must be considered for co-simulation purposes. The cooling system model must be solved within co-simulation time step to prevent missed deadlines and to remain in sync with RTS at all times. In the light of this, the numerical setting discussed in Section 5.2 must be carefully revised while expanding model capabilities and/or size, e.g., increasing the number of loads, zones,

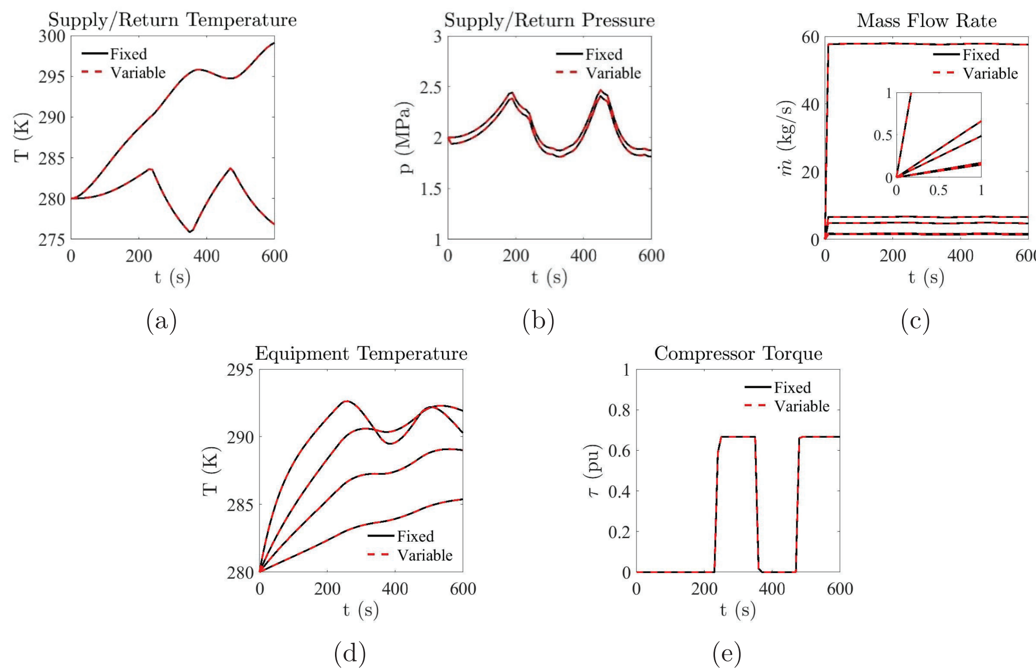

Figure 10: Comparison of variable-step and fixed-step solver results after configuring for real-time co-simulation.

etc. The scalability of the model discussed herein was evaluated to verify its suitability for modeling a notional four-zone MVDC ship cooling network with at least 50 shipboard equipment in addition to another 50 or more hydraulic components. Figure 11 shows the model scalability evaluated as the ratio of wall-clock time per simulation time with respect to the model size (number of shipboard loads).

The ratio of unity in Figure 11 is expected when it takes exactly one wall-clock second to advance one second in the simulation, i.e., the ratio of 0.5 implies that 0.5 wall-clock second is required to advance one simulation second. The ratio for the four-zone model with 53 shipboard components is approximately 0.68 on a Windows workstation with an Intel Core i7-6950 3.0 GHz CPU and 32 GB of 2666 MHz RAM. The ratio depends both on the available computational resources and simulation platform, yet in case of MATLAB/Simulink, similar ratios (between 0.5 and 0.7) have been obtained on other computers including Intel Xeon-4114 2.80 GHz and Core i9-9980HK with 32 GB of RAM. We thereby expect the complete model to run faster than wall-clock time during co-simulations on most workstations.

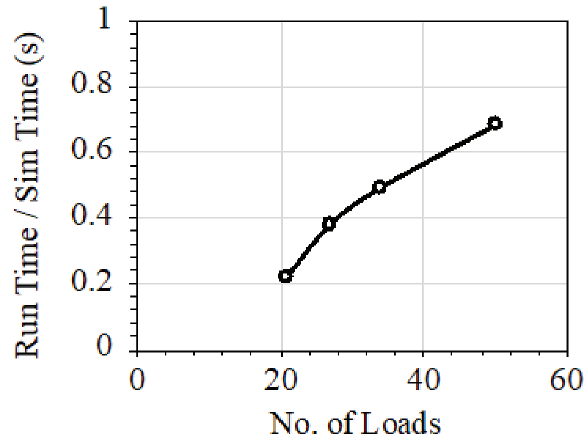

Figure 11: Model scalability evaluated as the ratio of wall-clock time / sim time.

5 Notional Model Parameters

This section summarizes the notional parameters defined for the proposed notional four-zone MVDC cooling system model illustrated in Figure 2. The cooling network is instrumented with temperature sensors and flow meters, placed at each load point, as well as pressure transducers placed at pump inlets and outlets. Currently, the cooling system is responsible for the operation of valves (gate valve, pressure-relief valve, and check valves) and chillers whose on-off cycles are determined by hysteresis control. In all cases, valves and chillers are controlled to ensure proper operation of all shipboard equipment within their design limits.

The piping network depicted in Figure 2 features cooling redundancy with cross-connected sides, i.e., starboard and port connected via supply and return headers. When the cooling demand on one side of ship becomes greater than its design capacity, the cross-connection allows for the allocation of extra cooling power, if any, from the other side. Similarly, interconnection of zones is underway as described in Section 3.4. Table 1 lists the cooling system design parameters applicable to all zones. The pump performance curve referenced by the model is depicted in Figure 6.

The valve openings in this particular model application are controlled by an ideal proportional-integral-derivative controller whose proportional, integral, and derivative values are -10^{-3}, 10^{-3}, and 10^{-4}, respectively. The upper and lower output saturation limits are set as the respective gate valve diameter and 10^{-12}, respectively. The lower limit is defined as nonzero to ensure numerical convergence.

Table 2 lists the thermal loads in all zones including dimensions, weight, rated electrical power (P_e), and efficiency (η_e). These load characteristics are provided as inputs to the generalized cooling system model along with the piping network characteristics de-

Table 1: Cooling system design parameters

Chillers	
Cooling capacity	2000 refrigeration tons
Coefficient of performance	3
Compressor speed, nominal	3570 RPM
Evaporator diameter	0.2 m
Evaporator length	200 m
Hysteresis	2 K
Setpoint chilled water temperature	280 K
Piping Network	
Expansion tank volume	5000 gal
Expansion tank pressure	0.6 MPa
Expansion tank valve set pressure	3 MPa
Header diameter	0.2 m
Header length, total	44 m
Supply header pressure, nominal	2 MPa
Pumps	
Power, nominal	18.64 kW
Speed, nominal	1750 RPM
Thermal Loads	
Design temperature	323.15 K
Heat exchanger diameter	0.1 m
Heat exchanger length	50 m
Valves	
Characteristic longitudinal length	0.1 m
Hydraulic diameter	0.1 m
Leakage area	10^{-12} m^2
Minimum opening area	10^{-12} m^2
K_P (Proportional)	-10^{-3}
K_I (Integral)	10^{-3}
K_D (Derivative)	10^{-4}

scribed in Table 1. The thermal load mass and specific heat have been approximated by assuming each component is only made of copper. Equivalent thermal properties (e.g., weight-averaged) may be used if the material composition of loads is known.

As described briefly in Section 3.3.1, the load profile for the present model can be provided in many different ways depending on the simulation mode (real-time co-simulation or standalone) and mission profile. We recommend testing the model first in an automated test framework wherein $\dot{Q}_s$ profiles are defined by tabulated time-dependent data, analytical functions, or constant values representing the dynamics of an SPS model. This will facilitate the verification of real-time co-simulation environment implementation by providing a reference case to compare against. The model user guide in Ref. [4] explains how the automated test framework can be setup for the proposed shipboard cooling system model.

The control and log signals relevant to thermal loads are flow control valve state (opened or closed), mass flow rate, and temperature, while those for the piping network include two additional signals, namely header pressure and cross-connection valve state. All signal names follow their corresponding to which relevant physical variable or unit is concatenated (note that each thermal load is named after its corresponding zone, side, and component type). For example, the temperature, mass flow rate, and flow control valve state of `z1_Port_ML1` in Table 2 are `z1_Port_ML1_K`, `z1_Port_ML1_kgps`, and `z1_Port_ML1_valve`, respectively, where `K` and `kgps` are units for temperature and mass flow rate. Similarly, STBD header supply and return pressure as well as the cross-connection (xC) valve state and mass flow rate are identified as `z1_STBD_HEADER_Supply_MPa`, `z1_STBD_HEADER_Return_MPa`, `z1_STBD_HEADER_xC_valve`, and `z1_STBD_HEADER_xC_kgps`, respectively.

This is the end of the MDD.

References

[1] ESRDC Team, "Notional four zone mvdc shipboard power/thermal-fluid system model." Available at https://www.esrdc.com/library/notional-four-zone-mvdc-shipboard-power-system-model.

[2] S. Yang, M. Chagas, and J. Ordonez, "Modeling, cross-validation, and optimization of a shipboard integrated energy system cooling network," *Applied Thermal Engineering*, vol. 145, pp. 516–527, 2018.

[3] MathWorks, *MATLAB 2020a*.

[4] ESRDC Team, "Notional four-zone mvdc shipboard cooling system model user guide." Available offlinel.

[5] COMSOL Inc., "COMSOL Multiphysics 5.5." https://www.comsol.com/.

A List of notional thermal loads

Table 2: List of notional thermal loads in all four zones

Name	Zone	Side	Length (m)	Width (m)	Height (m)	Weight (kg)	D_{pipe} (m)	L_{pipe} (m)	$\dot{Q}$ (MW)	T_{design} (K)
z1_Port_ACLC_Conv	1	Port	4	1.6	2.36	5,000	0.10	20.00	0.0554	323
z1_Port_ACLC_Vital	1	Port	1	1	1	8960	0.10	20.00	0.006	323
z1_Port_IPNC_Conv	1	Port	4	1.6	2.36	5,000	0.10	20.00	0.0554	323
z1_Port_MW	1	Port	1	1	1	8960	0.10	20.00	1.00005	323
z1_Port_IPNC_ML1	1	Port	6.8	5.08	7.7	56,000	0.10	20.00	0.12	323
z1_Port_IPNC_ESM	1	Port	2.17	1.9	1.51	15,000	0.10	20.00	0.34	323
z1_Port_PCM1A_Conv	1	Port	4	1.6	2.36	3,960	0.10	20.00	0.2128	323
z1_Port_PCM1A_ESM	1	Port	2.17	1.9	1.51	15,000	0.10	20.00	0.34	323
z2_STBD_IPNC_Conv	2	STBD	4	1.6	2.36	5,000	0.10	20.00	0.0626	323
z2_STBD_HRRL_CapBank	2	STBD	4	2	1	15,369	0.10	20.00	0.0716	323
z2_STBD_HRRL_ESM	2	STBD	2.17	1.9	1.51	15,000	0.10	20.00	0.34	323
z2_STBD_IPNC_ML2	2	STBD	4	1	4	10,000	0.10	20.00	0.375	323
z2_STBD_PCM1A_Conv	2	STBD	4	1.6	2.36	3,960	0.10	20.00	0.2128	323
z2_Port_PGM1_Conv1	2	Port	2.36	1.6	5.5	5,730	0.10	20.00	0.348	323
z2_STBD_PGM1_Conv2	2	STBD	2.36	1.6	5.5	5,730	0.10	20.00	0.348	323
z2_Port_PGM1_Generator	2	Port	4	3.81	14.3	97,045	0.10	20.00	5.8	323
z2_STBD_PGM2_Generator	2	STBD	4	3.81	14.3	97,045	0.10	20.00	5.8	323
z2_Port_PMM_Drive	2	Port	4.8	3.5	2.36	9,210	0.10	20.00	0.75	323
z2_STBD_ACLC_Conv	2	STBD	1	1	1	8960	0.10	20.00	0.008	323
z2_STBD_ACLC_Vital	2	STBD	1	1	1	8960	0.10	20.00	0.322	323
z2_STBD_IPNC_ESM	2	STBD	2.17	1.9	1.51	15,000	0.10	20.00	0.34	323
z2_STBD_MW	2	STBD	2	1	1	2,000	0.10	20.00	1.00005	323
z2_STBD_IPNC_ML1	2	STBD	0.6	2	2	1,000	0.10	20.00	0.195	323
z2_STBD_IPNC_ML3	2	STBD	2.5	1	2.5	2,500	0.10	20.00	0.12	323
z2_STBD_PCM1A_ESM	2	STBD	2.17	1.9	1.51	15,000	0.10	20.00	0.34	323
z2_Port_PGM2_Conv1	2	Port	2.36	1.6	5.5	5,730	0.10	20.00	0.348	323
z2_STBD_PGM2_Conv2	2	STBD	2.36	1.6	5.5	5,730	0.10	20.00	0.348	323
z2_STBD_PMM_Drive	2	STBD	4.8	3.5	2.36	9,210	0.10	20.00	0.75	323
z2_Port_PMM_Motor	2	Port	5.1	5.4	5.3	127,000	0.10	20.00	7.5	323
z3_Port_IPNC_Conv	3	Port	4	1.6	2.36	5,000	0.10	20.00	0.079	323
z3_Port_PCM1A_Conv	3	Port	4	1.6	2.36	3,960	0.10	20.00	0.1834	323
z3_Port_PGM3_Conv1	3	Port	2.36	1.6	5.5	5,730	0.10	20.00	0.348	323
z3_STBD_PGM3_Conv2	3	STBD	2.36	1.6	3.4	2,910	0.10	20.00	0.0448	323
z3_Port_PGM3_Generator	3	Port	4	3.81	14.3	97,045	0.10	20.00	5.8	323
z3_STBD_PGM4_Generator	3	STBD	2.39	2.36	7.14	27,273	0.10	20.00	0.74	323
z3_Port_PMM_Drive	3	Port	4.8	3.5	2.36	9,210	0.10	20.00	0.75	323
z3_STBD_ACLC_Conv	3	STBD	1	1	1	8960	0.10	20.00	0.008	323
z3_STBD_ACLC_Vital	3	STBD	1	1	1	8960	0.10	20.00	0.008	323
z3_STBD_IPNC_ESM	3	STBD	2.17	1.9	1.51	15,000	0.10	20.00	0.34	323
z3_STBD_MW	3	STBD	6.8	5.08	7.7	56,000	0.10	20.00	1.00005	323
z3_STBD_IPNC_ML1	3	STBD	1	1	1	8960	0.10	20.00	0.322	323
z3_STBD_PCM1A_ESM	3	STBD	2.17	1.9	1.51	15,000	0.10	20.00	0.34	323
z3_Port_PGM4_Conv1	3	Port	2.36	1.6	5.5	5,730	0.10	20.00	0.348	323
z3_STBD_PGM4_Conv2	3	STBD	2.36	1.6	3.4	2,910	0.10	20.00	0.0448	323
z3_STBD_PMM_Drive	3	STBD	4.8	3.5	2.36	9,210	0.10	20.00	0.75	323
z3_STBD_PMM_Motor	3	STBD	5.1	5.4	5.3	127,000	0.10	20.00	7.5	323
z4_STBD_ACLC_Conv	4	STBD	1	1	1	8960	0.10	20.00	0.008	323
z4_STBD_ACLC_Vital	4	STBD	1	1	1	8960	0.10	20.00	0.006	323
z4_STBD_IPNC_Conv	4	STBD	4	1.6	2.36	5,000	0.10	20.00	0.0398	323
z4_STBD_IPNC_ESM	4	STBD	2.17	1.9	1.51	15,000	0.10	20.00	0.34	323
z4_STBD_MW	4	STBD	6.8	5.08	7.7	56,000	0.10	20.00	1.00005	323
z4_STBD_IPNC_ML1	4	STBD	1	1	1	8960	0.10	20.00	0.302	323
z4_STBD_PCM1A_Conv	4	STBD	4	1.6	2.36	3,960	0.10	20.00	0.1834	323
z4_STBD_PCM1A_ESM	4	STBD	2.17	1.9	1.51	15,000	0.10	20.00	0.34	323
z4_Port_PGM5_Conv1	4	Port	2.36	1.6	3.4	2,910	0.10	20.00	0.0448	323
z4_STBD_PGM5_Generator	4	STBD	2.39	2.36	7.14	27,273	0.10	20.00	0.74	323
z4_STBD_PGM5_Conv2	4	STBD	2.36	1.6	3.4	2,910	0.10	20.00	0.0448	323